PHYSICAL REVIEW E **94**, 021201(R) (2016)

Disorder-induced heating of ultracold neutral plasmas created from atoms in partially filled optical lattices

D. Murphy and B. M. Sparkes*
School of Physics, The University of Melbourne, Victoria 3010, Australia
(Received 30 May 2016; published 8 August 2016)

We quantify the disorder-induced heating (DIH) of ultracold neutral plasmas (UCNPs) created from cold atoms in optical lattices with partial filling fractions, using a conservation of energy model involving the spatial correlations of the initial state and the equation of state in thermal equilibrium for a one-component plasma. We show, for experimentally achievable filling fractions, that the ionic Coulomb coupling parameter could be increased to a degree comparable to other proposed DIH-mitigation schemes. Molecular dynamics simulations were performed with compensation for finite-size and periodic boundary effects, which agree with calculations using the model. Reduction of DIH using optical lattices will allow for the study of strongly coupled plasma physics using low-density, low-temperature, laboratory-based plasmas, and lead to improved brightness in UCNP-based cold electron and ion beams, where DIH is otherwise a fundamental limitation to beam focal sizes and diffraction imaging capability.

DOI: 10.1103/PhysRevE.94.021201

Introduction. Ultracold neutral plasmas (UCNPs) created by photoionizing laser-cooled atoms are a platform for the study of strongly coupled matter, where interparticle interaction energy exceeds thermal kinetic energy. UCNPs provide a laboratory-based resource to study plasma behavior occurring in astrophysical environments, such as the dense high-temperature interiors of gas giants and in white-dwarf stars [1]. UCNPs are characterized by high values of the Coulomb coupling parameter

$$\Gamma = \frac{e^2}{4\pi\varepsilon_0 a k_B T}, \tag{1}$$

where e is the charge of one particle, ε_0 is the vacuum permittivity, the Wigner-Seitz radius $a = (3/4\pi n)^{1/3}$ is the average interparticle separation for particle density n, k_B is the Boltzmann constant, and T is the particle temperature. Γ is the ratio of the interparticle Coulomb potential and kinetic energy. Strong coupling occurs when $\Gamma > 1$, indicating that particle motion within the plasma is dominated by interparticle forces, giving rise to collective effects that result in Wigner crystallization for $\Gamma > 174$ [2]. Strongly coupled UCNPs are also potentially useful as a source of highly focusable electrons and ions suitable for high-resolution coherent diffraction imaging and microscopy [3,4].

When cold atoms in a magneto-optical trap (MOT) are photoionized to produce a UCNP, minimal kinetic energy is imparted by the ionizing laser to the ions and electrons, giving velocity spreads equivalent to less than 1 mK and 10 K, respectively [5]. The low initial temperatures would imply strong coupling for the ions, but UCNP studies have not been able to reach far into the strongly coupled regime due to the disorder-induced heating (DIH) effect [6]. DIH arises from thermalization of random initial interparticle potentials because the ions are created from atoms that have an irregular spatial distribution. The ions gain kinetic energy through mutual Coulomb repulsion, oscillating about dynamic local potential minima at the plasma frequency $\omega = \sqrt{ne^2/\varepsilon_0 m}$, where m is the ion mass, and oscillating in kinetic energy at a frequency of 2ω. Thermalization to an equilibrium coupling parameter $\Gamma_{eq} \sim 1$ occurs in times on the order of one plasma period $2\pi/\omega$ as the kinetic energy oscillations dephase. DIH limits charged particle beam brightness, which is directly proportional to Γ, as particle spatial distributions are uncorrelated at a conventional beam source [7].

In principle, DIH can be suppressed in UCNPs by preparing atoms with spatial correlations prior to ionization, such as in Fermi-degenerate or blockaded Rydberg gases [8,9], which have interatomic interactions that place lower limits on the nearest-neighbor spacings. It has also been predicted that DIH can be entirely prevented in UNCPs created from atoms trapped in optical lattices, which have a crystal-like structure formed in the interference of high-intensity laser beams, if single atoms occupy a high fraction ($f > 0.99$) of the lattice sites [10]. Achieving high filling fractions is experimentally challenging, however, models and simulations to date have not predicted Γ_{eq} for lattice-correlated UCNP at filling fractions $f < 0.99$. Preparation of single atoms in lattice sites is typically limited to $f \leqslant 0.5$, as sites initially holding more than one atom depopulate via pairwise collisions, resulting in an equal probability of being occupied or being vacant [11]. Filling fractions exceeding 0.5 can be achieved through a transition to a Mott insulating state in a condensed gas [12]. It may also be possible to exceed $f = 0.5$ through coherent excitation (and subsequent ionization) of Rydberg atoms to quasicrystalline spatial distributions within a lattice [13].

In this Rapid Communication we calculate the equilibrium Coulomb coupling parameter of UCNPs undergoing DIH created from partially filled ($0 < f < 0.99$) optical lattices. The model is compared to molecular dynamics simulations performed in periodic boundary conditions, accounting for the finite-size effects. Predicting the equilibrium properties of UCNPs as a function of experimental parameters will enable future experiments to target the most promising conditions for obtaining strong coupling for astrophysical simulations [14]. Increased coupling in UCNPs will also enable increased brightness in ion beams extracted from cold atom sources, which serve as a platform for the study of intrabeam Coulomb

*bsparkes@unimelb.edu.au

interactions relevant to future generations of charged particle beam sources [15,16].

Lattice heating calculations. The equilibrium value of the Coulomb coupling parameter after DIH, and its increase through correlations, can be calculated using conservation of energy between the potential energy of the initial lattice distribution and the thermal and binding energy of the equilibrium distribution of a strongly coupled plasma. We model a nonexpanding one-component plasma (OCP), infinite in spatial extent, where electrons in the plasma form a neutralizing background for the ions. Expanding UCNPs do not reach an equilibrium, with Γ increasing in time as a function of system size following DIH [17]. However, the ratio of the coupling parameters for a correlated to a disordered system with expansion is equal to that for a nonexpanding system [16]. Therefore, calculation of Γ as a function of the correlation parameter f quantifies the suppression of DIH independent of the expansion, which depends on the plasma dimensions, and on the electron temperature. The OCP description of a UCNP assumes that the electrons are weakly coupled at high temperature, with no influence on the ion interactions. For UCNPs with low-temperature electrons, inter-ion interactions are reduced to a Yukawa-type potential [18], but, with a generalized definition of Γ including the reduced potential, it can be shown that $\Gamma_{\rm eq}$ is not dependent on the electron temperature [19]. We assume that the UCNP is created in times much less than the DIH time scale ($2\pi/\omega$), which can be achieved using ultrafast photoionizing lasers or pulsed external electric fields [9].

The initial internal binding energy per particle of a system of charged particles with Wigner-Seitz radius a occupying a fraction f of the sites of a lattice is

$$u_{\rm i} = -\frac{e^2}{4\pi\varepsilon_0 a}\frac{f^{2/3}M}{2}, \tag{2}$$

which is f times the Madelung energy of a lattice with Madelung constant M and charge e at each site [20]. An additional factor of $f^{-1/3}$ is included to take into account the average interparticle separation a of only the occupied lattice sites. Atoms with initial temperature $T_{\rm i}$ in lattice sites with harmonic trapping frequency ν are displaced from the lattice sites by standard deviation $\sigma = \sqrt{k_{\rm B}T_{\rm i}/m(2\pi\nu)^2}$ in each axis. Atomic displacement due to thermal motion reduces the initial binding of the ions compared to the zero-temperature case by a value that can be written for small displacements, to first order in the dimensionless quantity $(\sigma/a')^2$, where $a' = f^{1/3}a$ is the Wigner-Seitz radius for the lattice sites, as [10]

$$\Delta = \frac{e^2}{4\pi\varepsilon_0 a}\frac{3f^{2/3}}{2}\left(\frac{\sigma}{a'}\right)^2, \tag{3}$$

which includes the scaling by f as in Eq. (2). The initial energy per particle of the ions is the sum of the binding energy $u_{\rm i}$, the displacement energy Δ, and the initial kinetic energy $k_{\rm i} = 3k_{\rm B}T_{\rm i}/2$.

The binding energy in thermal equilibrium for the strongly coupled fluid phase, occurring for $1 < \Gamma_{\rm eq} < 170$, is

$$u_{\rm eq} = -\frac{e^2}{4\pi\varepsilon_0 a}\left(A + B\,\Gamma_{\rm eq}^{-2/3} + C\,\Gamma_{\rm eq}^{-1}\right), \tag{4}$$

where the factor $A = 0.9$ gives the lower bound to the OCP energy [21] and factors $B = -0.590\,673$ and $C = 0.265\,69$ are given by fits of a known form of the OCP equation of state to simulation data [22]. The total energy per particle in equilibrium is $u_{\rm eq}$ plus the equilibrium kinetic energy written in terms of the equilibrium coupling parameter as $k_{\rm eq} = 3e^2/8\pi\varepsilon_0 a\Gamma_{\rm eq}$.

Equating the initial and equilibrium energies, excluding the relatively small $k_{\rm i}$, results in the expression

$$\frac{1}{2}f^{2/3}\left[M - 3\left(\frac{\sigma}{a'}\right)^2\right] = A + B\,\Gamma_{\rm eq}^{-2/3} + \left(C - \frac{3}{2}\right)\Gamma_{\rm eq}^{-1}, \tag{5}$$

from which $\Gamma_{\rm eq}$ can be calculated in terms of M, f, and σ/a'. At typical UCNP ion densities of $n = 10^{16}$ m^{-3} and initial temperatures $T_{\rm i} < 1$ mK, exclusion of $k_{\rm i}$ has a negligible effect for $f < 0.99$, so that $\Gamma_{\rm eq}$ can be calculated with only the dimensionless quantities of Eq. (5).

Molecular dynamics simulations. We simulated DIH for ^{85}Rb ions (mass $m = 1.41 \times 10^{-25}$ kg) in partially filled lattices of simple cubic (sc), face-centered-cubic (fcc), and body-centered-cubic (bcc) geometries, which are experimentally realizable with suitable choices of laser geometry [23–25], and have Madelung constants $M_{\rm sc} = 1.760\,12$, $M_{\rm fcc} = 1.791\,75$, and $M_{\rm bcc} = 1.791\,86$, respectively [26]. Molecular dynamics simulations were initialized with ion positions set at lattice sites for a range of filling fractions, choosing the cubic lattice dimensions so that the number of ions N was closest to 1000 for consistency. Ion density in simulation was kept constant at $n = 10^{16}$ m^{-3} by varying the lattice spacing, giving one-to-one correspondence between the temperature and coupling parameter across our simulations. Experimentally, lattice spacings are fixed by the laser wavelength and geometry so that low filling fractions will typically correspond to low density, but our main result in predicting $\Gamma_{\rm eq}$ as a function of f is dimensionless and independent of density. Figure 1(a) shows a two-dimensional representation of the initial positions for ions of different filling fraction but equal density.

Ions from lattice-trapped atoms with thermal displacement were simulated for a trapping frequency of $\nu = 15$ kHz. Each particle was assigned a random velocity using a Gaussian thermal distribution, for the chosen σ/a' parameter, and a random phase for the oscillatory harmonic motion in each axis, which together define a spatial displacement relative to the lattice site. For simplicity, we assume that photoionization is instantaneous, though we observe negligible differences in the equilibria of simulations repeated with ionization times up to 7 ns, or 1.6×10^{-2} times the DIH time scale, typical of the duration of pulsed lasers used to ionize atoms in a UCNP.

Equations of motion for the set of $\mathbf{N} = \{1,2,\ldots,N\}$ ions with positions $\mathbf{x}_{i\in\mathbf{N}}$, interacting via Coulomb forces in cubic periodic boundaries, were taken from the gradient of Ewald-summed interparticle potentials [27,28], splitting the calculation into two separately convergent sums of the interparticle forces as

$$\frac{d^2\mathbf{x}_i}{dt^2} = \frac{1}{m}\left(\mathbf{F}_i^{(1)} + \mathbf{F}_i^{(2)}\right). \tag{6}$$

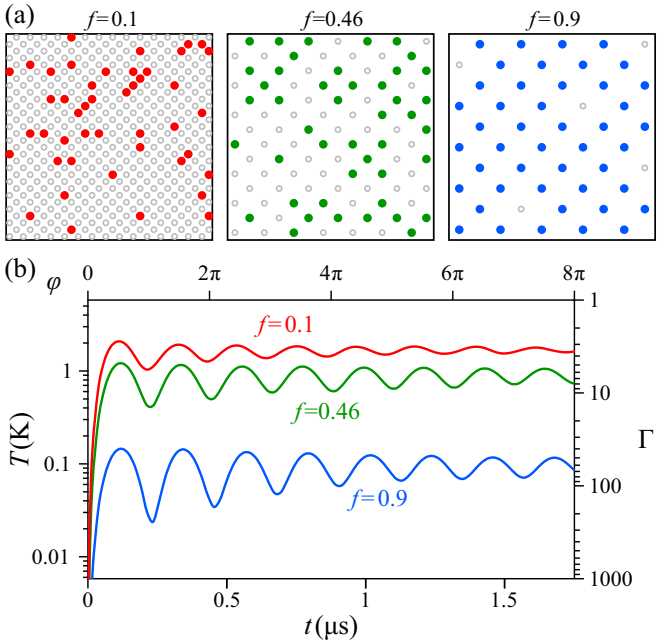

FIG. 1. (a) Two-dimensional lattices with different filling fraction f but equal atom density. The solid circles represent the position of atoms, and the open circles represent vacant lattice sites. (b) Simulations of disorder-induced heating in ionized rubidium atoms located at the sites of a three-dimensional body-centered-cubic lattice with filling fraction f. All simulations have equal density, allowing a direct comparison of temperature T to the coupling parameter Γ, and time following ionization t to the plasma phase $\varphi = \omega t$. Lattices of high filling fraction equilibrate to lower temperature and higher coupling parameter, reflecting increased interparticle spatial correlations in the initial distribution.

The Ewald method shields the long-ranged, positive-valued ionic Coulomb potentials with Gaussian negative-charge distributions of standard deviation γ, allowing a convergent sum of the shielded forces in real space,

$$\mathbf{F}_i^{(1)} = \frac{e^2}{4\pi\varepsilon_0}\sum_{j\neq i}\sum_{\mathbf{n}}\frac{\mathbf{r}_{i,j\mathbf{n}}}{|\mathbf{r}_{i,j\mathbf{n}}|^3}\left[\operatorname{erfc}\left(\frac{|\mathbf{r}_{i,j\mathbf{n}}|}{\sqrt{2}\gamma}\right) + \sqrt{\frac{2}{\pi}}\frac{|\mathbf{r}_{i,j\mathbf{n}}|}{\gamma}\exp\left(-\frac{|\mathbf{r}_{i,j\mathbf{n}}|^2}{2\gamma^2}\right)\right]. \quad (7)$$

Equation (7) uses the complementary error function $\operatorname{erfc}(z) = 1 - \operatorname{erf}(z)$, taken over all $j \neq i$ ions for cubic-boundary lattice vectors $\mathbf{n} \in \mathbb{Z}^3$ with separation vectors $\mathbf{r}_{i,j\mathbf{n}} = \mathbf{x}_i - (\mathbf{x}_j + \mathbf{n}L)$, where the boundary length is $L = (N/n)^{1/3}$ for a simulation of N ions at density n. The contributions to the forces from the negative shielding potentials are counteracted by adding equally placed positive-charge Gaussian potentials and taking the sum of forces in reciprocal space,

$$\mathbf{F}_i^{(2)} = \frac{2e^2}{4\pi\varepsilon_0 L^2}\sum_{j\neq i}\sum_{\mathbf{h}\neq\mathbf{0}}\frac{\mathbf{h}}{|\mathbf{h}|^2}\exp\left[-2\left(\frac{\gamma\pi}{L}\right)^2|\mathbf{h}|^2\right] \times \sin\left(\frac{2\pi}{L}\mathbf{h}\cdot\mathbf{r}_{i,j\mathbf{0}}\right), \quad (8)$$

over the reciprocal lattice vectors $\mathbf{h} \in \mathbb{Z}^3$ of the simple-cubic periodic boundary. We used the approximation of Ref. [29] where the sums converge for the choice of parameters $\gamma = L/\sqrt{2}$ with sums over $\mathbf{n}$ so that $|\mathbf{r}_{i,j\mathbf{n}}| \leqslant 2.6L$, and $|\mathbf{h}| \leqslant 8$. Once initialized, the equations of motion were integrated using the Bulirsch-Stoer method with polynomial-function extrapolation [30] with respect to the dimensionless plasma phase $\varphi = \omega t$, where t is the time following ionization. The maximum integral step in the plasma phase was limited to $0.05 \times 2\pi$ in order to resolve the kinetic energy oscillations [seen in Fig. 1(b)].

Simulations are affected by the finite size of the periodic boundaries, as the repeating images of the system introduce effective correlations into the ion position distribution at the scale of the boundary length [31]. In the initial binding energy calculation of Eq. (2) it is assumed that the lattice vacancies are distributed randomly, but the periodic boundary conditions give the vacancies a simple-cubic repeating structure. Each ion that is "removed" from a lattice site under periodic boundaries causes the remaining ions to retain one unit of simple-cubic binding energy relative to the removal of an equivalent fraction of ions from an infinite distribution. This residual binding energy can be accounted for by introducing an additional term in the calculation of the initial energy

$$u_{\mathrm{PBC}} = -\frac{e^2}{4\pi\varepsilon_0 a}\frac{(1-f)M_{\mathrm{sc}}}{2N^{1/3}}, \quad (9)$$

which is the vacant fraction lattice energy for the simple-cubic structure of the periodic boundaries, for a simulated ion number N.

Calculations of Γ_{eq} including the boundary-correction term (9) in the initial energy of the system can accurately predict the results of the simulations with finite-size effects. Instead, to give results for a system without periodic boundary conditions, we compensate for the finite-size effects by using a correction factor for the coupling parameter evaluated in the simulations. The correction factor is equal to the expected factor by which the prediction of Γ_{eq} for a finite-sized system would differ from the prediction of Γ_{eq} for an infinite system with $u_{\mathrm{PBC}} \to 0$. Simulations for different lattice geometries and filling fractions differ slightly in ion number N due to the cubic scaling of N with lattice dimensions, and therefore also differ in correction factor.

Examples of simulations of ions with zero initial temperature created in a three-dimensional bcc lattice with different filling fractions are shown in Fig. 1(b), corrected for the influence of the periodic boundaries. The ion temperature is plotted against time following ionization, or in dimensionless terms plotted for the coupling parameter against plasma phase φ, exhibiting the damped kinetic energy oscillations expected of an equilibrating UCNP. Ions with a high lattice filling fraction equilibrate to a lower temperature and higher coupling parameter than ions with a low filling fraction, reflecting the increased initial correlations.

Results and discussion. The equilibrium coupling parameter Γ_{eq} was evaluated from the simulations by taking the average of the periodicity-corrected coupling parameters at each time step between plasma phases 8π and 16π. Figure 2 shows the simulated results for zero initial temperature ions

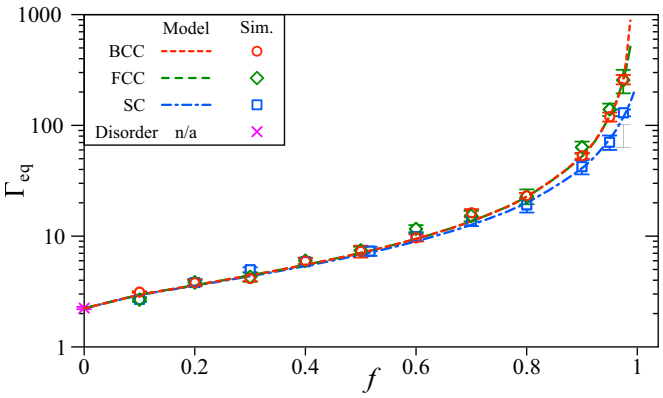

FIG. 2. Calculated (lines) and simulated (points) equilibrium coupling parameters Γ_{eq} for body-centered-cubic (bcc), face-centered-cubic (fcc), and simple-cubic (sc) lattices at different atomic filling fractions f, for atoms of zero initial temperature. High filling fractions lead to increased coupling parameter Γ_{eq} in equilibrium compared to random placement (disorder), which is equivalent to $f = 0$. Γ_{eq} was evaluated in simulation over plasma phases φ between 8π and 16π, with uncertainty as one standard deviation in that period. Differences in Γ_{eq} between lattices result from the different binding energies in the initial state, with the bcc and fcc lattices reaching higher coupling than the sc lattice at fixed f.

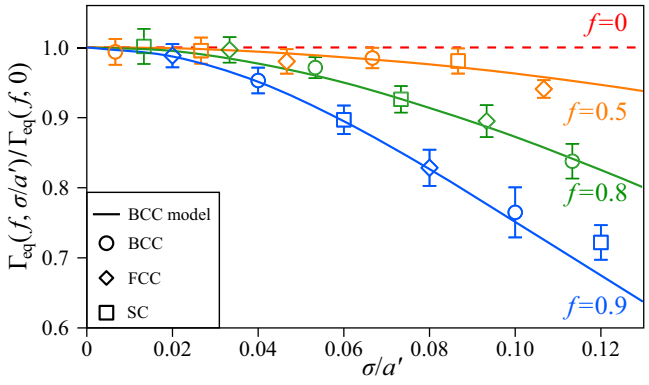

FIG. 3. Lowering of the equilibrium coupling parameter due to thermal broadening of lattice sites, expressed as the ratio of the equilibrium coupling parameters for displaced to nondisplaced atoms in lattices with filling fraction f. The atomic displacement σ is normalized to the Wigner-Seitz radius a' for the lattice sites. Simulations (data points) are performed for the simple-cubic (sc), face-centered-cubic (fcc), and body-centered cubic (bcc) lattices at different filling fractions, averaging the ratios over the evaluation period between plasma phases of 8π and 16π with error bars as one standard deviation, and the theoretical calculations (solid lines) are shown for the bcc lattice only.

($\sigma/a' = 0$) for the body-centered-, face-centered-, and simple-cubic lattices at different filling fractions. These give strong agreement to the theoretical predictions for the dependence of the equilibrium coupling parameter on the filling fraction for each lattice, and to the results for a disordered distribution with randomly placed ions, equivalent to a lattice with $f = 0$, which has $\Gamma_{eq} = 2.2$. Uncertainties in the simulation data result from residual kinetic energy oscillations during the evaluation period for Γ_{eq}. The bcc and fcc lattice results are similar, owing to their nearly equal Madelung constants, while the sc lattice tended to have lower Γ_{eq} at high values of f due to its lower Madelung constant.

Ions with initial thermal displacement from the lattice sites have lowered Γ_{eq} compared to ions from lattices of the same f with zero initial temperature, as the displacements reduce the initial interparticle correlations. Figure 3 shows theoretical predictions and simulation results for the factor by which Γ_{eq} for thermally displaced atoms is reduced compared to the zero-temperature result. The data points are the averages of the coupling parameter ratios for the displaced and zero-temperature simulations at each time step over the $8\pi < \varphi < 16\pi$ evaluation period, with uncertainties as one standard deviation. Simulations were performed for the sc, fcc, and bcc lattices, however, we only show the predictions for the bcc lattice as the ratios are not strongly dependent on the Madelung constant. Thermal displacements have a greater impact on Γ_{eq} for lattices of high f, reducing the otherwise high spatial correlations, than for lattices of low f. For example, distributions with $f = 0$ gain no additional disorder when the atoms are displaced. The simulations agreed with the predictions up to $\sigma/a' = 0.1$, a relatively high parameter for lattice-trapped atoms. For example, the experiments of Ref. [32] achieve $\sigma/a' = 0.087$ for cesium atoms at 10 μK in a 4.9 μm site-separation ($a' = 3.0$ μm) simple-cubic lattice with trapping frequency $\nu = 15$ kHz.

A UCNP created from the above example SC lattice with $\sigma/a' = 0.087$, at the typical experimental limit of $f = 0.5$, would have $\Gamma_{eq} = 6.7$, compared to $\Gamma_{eq} = 2.2$ for disordered atoms. Our results show that by creating UCNP from optical-lattice trapped atoms, even with imperfect filling fraction, an increase in Γ_{eq} may be achieved that is comparable to the expected increases using doubly ionized [33] or Rydberg-blockade correlated atoms [9,16]. Achieving an increase in Γ_{eq} by greater than an order of magnitude compared to disordered ions would require $f > 0.8$ and cooling of the atoms to near the vibrational ground state of the lattice trapping potential.

Conclusion. In summary, we have shown that the coupling parameter in ultracold neutral plasmas can be increased by spatially correlating the cold atoms, prior to ionization, using an optical lattice even with imperfect filling. We have presented a model for calculating the equilibrium coupling parameter following disorder-induced heating of lattice-correlated ions as a function of the lattice geometry, filling fraction, and initial atomic temperature. Calculations using the model are consistent with detailed molecular dynamics simulations, when the additional correlations resulting from periodic boundary effects are accounted for. Increased coupling parameters will allow for observation of strongly coupled plasma processes using UCNP, and will increase the brightness of cold ion beams using the UCNP source beyond the otherwise fundamental limit imposed by disorder-induced heating.

Acknowledgments. We acknowledge helpful discussions with R. E. Scholten. B.M.S. gratefully acknowledges the support of a University of Melbourne McKenzie Fellowship. This work was supported by the Australian Research Council Discovery Project No. DP140102102.

[1] T. C. Killian, Science **316**, 705 (2007).
[2] S. Ichimaru, Rev. Mod. Phys. **54**, 1017 (1982).
[3] B. J. Claessens, S. B. van der Geer, G. Taban, E. J. D. Vredenbregt, and O. J. Luiten, Phys. Rev. Lett. **95**, 164801 (2005).
[4] J. L. Hanssen, E. A. Dakin, J. J. McClelland, and M. Jacka, J. Vac. Sci. Technol. B **24**, 2907 (2006).
[5] T. C. Killian, S. Kulin, S. D. Bergeson, L. A. Orozco, C. Orzel, and S. L. Rolston, Phys. Rev. Lett. **83**, 4776 (1999).
[6] D. O. Gericke and M. S. Murillo, Contrib. Plasma Phys. **43**, 298 (2003).
[7] J. M. Maxson, I. V. Bazarov, W. Wan, H. A. Padmore, and C. E. Coleman-Smith, New J. Phys. **15**, 103024 (2013).
[8] M. S. Murillo, Phys. Rev. Lett. **87**, 115003 (2001).
[9] G. Bannasch, T. C. Killian, and T. Pohl, Phys. Rev. Lett. **110**, 253003 (2013).
[10] T. Pohl, T. Pattard, and J. M. Rost, J. Phys. B: At. Mol. Opt. Phys. **37**, L183 (2004).
[11] M. T. DePue, C. McCormick, S. L. Winoto, S. Oliver, and D. S. Weiss, Phys. Rev. Lett. **82**, 2262 (1999).
[12] J. F. Sherson, C. Weitenberg, M. Endres, M. Cheneau, I. Bloch, and S. Kuhr, Nature (London) **467**, 68 (2010).
[13] J. Schachenmayer, I. Lesanovsky, A. Micheli, and A. J. Daley, New J. Phys. **12**, 103044 (2010).
[14] D. Comparat, T. Vogt, N. Zahzam, M. Mudrich, and P. Pillet, Mon. Not. R. Astron. Soc. **361**, 1227 (2005).
[15] D. Murphy, R. W. Speirs, D. V. Sheludko, C. T. Putkunz, A. J. McCulloch, B. M. Sparkes, and R. E. Scholten, Nat. Commun. **5**, 4489 (2014).
[16] D. Murphy, R. E. Scholten, and B. M. Sparkes, Phys. Rev. Lett. **115**, 214802 (2015).
[17] T. Pohl, T. Pattard, and J. M. Rost, Phys. Rev. Lett. **94**, 205003 (2005).
[18] T. K. Langin, T. Strickler, N. Maksimovic, P. McQuillen, T. Pohl, D. Vrinceanu, and T. C. Killian, Phys. Rev. E **93**, 023201 (2016).
[19] M. Lyon, S. D. Bergeson, and M. S. Murillo, Phys. Rev. E **87**, 033101 (2013).
[20] The total electrostatic energy of a lattice where the charge is reduced by a factor of f scales as f^2, but this energy is shared between only the sites containing charge, so the energy per charged particle scales as f.
[21] M. Baus and J. P. Hansen, Phys. Rep. **59**, 1 (1980).
[22] D. H. E. Dubin and T. M. O'Neil, Rev. Mod. Phys. **71**, 87 (1999).
[23] I. Bloch, Nat. Phys. **1**, 23 (2005).
[24] G. Grynberg, B. Lounis, P. Verkerk, J.-Y. Courtois, and C. Salomon, Phys. Rev. Lett. **70**, 2249 (1993).
[25] C. S. Adams, S. G. Cox, E. Riis, and A. S. Arnold, J. Phys. B: At. Mol. Opt. Phys. **36**, 1933 (2003).
[26] R. M. Martin, *Electronic Structure: Basic Theory and Practical Methods* (Cambridge University Press, Cambridge, UK, 2004).
[27] C. Kittel and P. McEuen, *Introduction to Solid State Physics* (Wiley, New York, 1986).
[28] L. Hernquist, F. R. Bouchet, and Y. Suto, Astrophys. J. Suppl. Ser. **75**, 231 (1991).
[29] M. J. L. Sangster and M. Dixon, Adv. Phys. **25**, 247 (1976).
[30] W. H. Press *et al.*, *Numerical Recipes in C* (Cambridge University Press, Cambridge, UK, 2012).
[31] G. Makov and M. C. Payne, Phys. Rev. B **51**, 4014 (1995).
[32] K. D. Nelson, X. Li, and D. S. Weiss, Nat. Phys. **3**, 556 (2007).
[33] M. Lyon and S. D. Bergeson, Contrib. Plasma Phys. **55**, 399 (2015).